Desalination and Water Treatment
www.deswater.com

doi: 10.1080/19443994.2014.932710

56 (2015) 121–135
September

Taylor & Francis
Taylor & Francis Group

Decolorization of Reactive Black 5 by persulfate oxidation activated by ferrous ion and its optimization

Tunlawit Satapanajaru[a,b,*], Maneekarn Yoo-iam[a], Pinnaree Bongprom[a], Patthra Pengthamkeerati[a,b]

[a] *Faculty of Environment, Department of Environmental Technology and Management, Kasetsart University, Bangkok 10900, Thailand, Tel. +662-579-3877; emails: fscitus@ku.ac.th (T. Satapanajaru), ymaneekarn@gmail.com (M. Yoo-iam), Tel. +683-541-5627; email: bongpinnaree@gmail.com (P. Bongprom), Tel. +662-579-3877; email: fsciptp@ku.ac.th (P. Pengthamkeerati)*
[b] *Environmental Technology Special Research Unit, Kasetsart University, Bangkok 10900, Thailand*

Received 21 December 2013; Accepted 3 June 2014

ABSTRACT

We determined the effectiveness of persulfate (PS) activated by Fe^{2+} to treat Reactive Black 5 (RB5) dye. The experimental variables of persulfate dosage, Fe^{2+} dosage, initial dye concentration, solution pH, activators, and NaCl were investigated. The complete decolorization of RB5 by 200 mM PS activated by 1 mM Fe^{2+} was 100% within 12 h but the TOC removal efficiency was only 70% within 24 h. When the PS dosage and Fe^{2+} dosage increased, the k_{obs} of RB5 decolorization increased. On the other hand, when the initial RB5 concentration increased from 0.01 to 0.05 mM and concentration of PS was fixed at 400 mM, the number of sulfate radicals did not increase proportionally, so the k_{obs} of the RB5 decolorization decreased. Lowering the pH from 11 to 5 increased the kinetic rates of destruction of RB5. At a higher pH, the concentration of Fe^{2+} could decrease due to the formation of iron oxides which hinder the further reaction of Fe^{2+} with PS. Five activators (Fe^0, Fe^{2+}, Fe^{3+}, Ag^0, and Ag^+) were chosen to study their capability in activating PS oxidation. At the equivalent mole of activator, the k_{obs} of the treatment of PS activated by Fe^0 was the best (2.8609 h^{-1}). Increasing the NaCl concentration from 17.24 mM (1g L^{-1}) to 68.96 mM (4 g L^{-1}) decreased the kinetic removal rates of RB5. The PS oxidation of RB5 was optimized using response surface methodology. The interactive effects of three factors namely, persulfate dosage (X_1), Fe^{2+} dosage (X_2), and pH (X_3) were investigated. The results indicated the optimum condition to treat 0.01 mM RB5 to be 445 mM PS and 4.91 mM Fe^{2+} at pH 5.45.

Keywords: Decolorization; Ferrous ion; Persulfate; Reactive Black 5; Response surface methodology (RSM)

1. Introduction

Azo dyes are characterized by presenting one or more azo bonds (–N=N–) which are widely used in several industries, especially textile dyeing mills. Most azo dyes are complex aromatic structures, which are difficult to be decayed by natural attenuation processes. Many organic dyes are hazardous and may affect aquatic life and even the food chain [1,2]. There are many physical, chemical, and biological methods for dye removal: chemical coagulation, flocculation, chemical

---

*Corresponding author.

oxidation [3], chemical reduction [4], adsorption [5], photochemical oxidation [6], membrane filtration [7], and aerobic/anaerobic biological degradation [8]. All of these methods suffer from one or more limitations, and none of them are able to remove dyes completely from wastewater [9]. Moreover, some methods may generate highly toxic secondary products [10]. Advanced oxidation processes (AOPs) have been developed to oxidize azo dyes in wastewater. AOPs are based on generating radicals such as the hydroxyl radical ($^{\cdot}OH$) or the sulfate radical ($SO_4^{-\cdot}$) which can destroy a broad range of organic pollutants quickly and non-selectively [3,11]. Radical species can be formed in homogeneous systems via electron transfer by transition metal activation of the oxidants such as hydrogen peroxide (H_2O_2), persulfate (PS), peroxymonosulfate (PMS), etc. [12].

Persulfate (PS, $S_2O_8^{2-}$) is a strong oxidizing agent with a high redox potential (2.05 V) and it has been used widely in the petroleum industry for the treatment of hydraulic fluids or as a reaction initiator [13]. PS is non-selectively reactive, and it is relatively stable at room temperature [14]. With the activation of UV, heat, or transition metals (M) such as Fe^{2+}, Fe^{3+}, etc. persulfate can form more powerful sulfate free radicals ($SO_4^{-\cdot}$), which have a higher redox potential (2.4 V) [15,16]. Among the known oxidants used in wastewater treatment, only $^{\cdot}OH$ radicals have potentials ($E = 2.72$ V) close to $SO_4^{-\cdot}$ radicals [17]. The half-cell reaction of sulfate free radicals is shown in Eq. (1):

$$SO_4^{-\cdot} + e^- \rightarrow SO_4^{2-} \qquad E_0 = 2.4\,\text{V} \tag{1}$$

The activation by transition metals is the most variable method for the field application of this oxidation method, because thermal activation would require heating the treatment system which poses significant engineering challenges and is not cost effective, and for UV activation, the wastewater needs to be pumped out for passage through UV reactor, which also adds cost and complexity [18]. Many transition metals for example, Ag^+, Ce^{3+}, Co^{2+}, Fe^{2+}, Fe^{3+}, Mn^{2+}, Ni^{2+}, Ru^{3+}, and V^{3+} could activate PS to generate SO_4 radicals [19]. Iron has been widely used as a transition metal because it is relatively inexpensive, non-toxic, and effective [20]. Moreover, the use of zerovalent iron (Fe^0) instead of iron salts (Fe^{2+}, Fe^{3+}) prevents any additional anion loading in the wastewater treatment [21]. Zerovalent iron undergoes oxidation in water to give $Fe^{2+,}$ then Fe^{2+} also reacts with water, generating Fe^{3+}. When Fe^{3+} reacts with the persulfate anion, two molecules of sulfate radicals are produced as shown in Eq. (2):

$$S_2O_8^{2-} + Fe^{3+} \rightarrow Fe^{2+} + SO_4^{2-} + SO_4^{-\cdot} \tag{2}$$

It has also been reported to be effective for degrading some azo dyes contained in synthetic wastewater, such as Methylene Blue [22,23], Acid Orange 7 [3,24], Cibacron Brilliant Yellow 3 [10], Sunset Yellow, and Ponceau 4R [25]. Sulfate radicals can oxidize the azo bond (–N=N–) in the chromophore of dyes. The destruction of the azo bond leads to the decolorization of the dye solution [2]. Beside dyes, salt, especially NaCl, was used in textile dyeing process. Vishnu et al. [26] indicated that about 600–700 ton of fabrics was processed requiring 400–500 ton of salt. This generated the large quantity of total dissolved solids and chlorides in wastewater. The estimated concentration of chloride was in the range of 2,000–3,500 mg L^{-1}. This ion increases the ionic strength of the medium and thus, may affect the catalytic activity in physicochemical wastewater treatment [6]. In oxidation of RB5 by UV/TiO_2, addition of NaCl favored partitioning of RB5 to the TiO_2 surface, increasing adsorption of RB5, then decolorization was thus accelerated [6].

Generally, wastewater treatments by chemical methods are optimized using a "one at a time strategy" of the treatment parameter, so it is time consuming and may ignore the combined interactions between parameters [27,28]. As a solution, the statistical method of response surface methodology (RSM) has been proposed to include the influence of individual factors as well as their interactive influences [29]. RSM has been used to optimize wastewater processes such as the coagulation–flocculation process of leachate treatment [29], the photodecolorization of the sulfonated diazo dye Reactive Green 19 [30], the photoelectrocatalytic oxidation of fulvic acid [27], and the photoinduced decolorization of toludine blue [31]. However, a few studies were reported to optimize the decolorization of dyes by PS oxidation.

In this study, Reactive Black 5 (RB5) was investigated because RB5 is commonly found at a higher concentration than other reactive dyes in dyebath effluents [6]. Even though the decolorization of RB5 was studied using various oxidants, we lack the information of RB5 decolorization by PS/various activators. To date, there have only been a few attempts to propose the possible product of the decolorization products of RB5. Furthermore, we used the mathematical and statistical techniques for analyzing the effects of independents variables on RB5 oxidation by PS and investigating its optimal condition. We quantified the decolorization effectiveness of RB5 in synthetic wastewater by PS oxidation. We also examined the effects of the ratio of PS to Fe^{2+} (activator), initial dye concentration, solution pH, and transition metal, (Fe^0, Fe^{2+}, Fe^{3+}, Ag^0, and Ag^+) on the decolorization rates of RB5. Moreover, we determined the effects of NaCl on the destruction of RB5 by PS oxidation. Statistics-based experimental design with RSM was also employed to investigate the optimization of the decolorization of RB5 by PS oxidation.

2. Experimental procedures

2.1. Materials

Reactive Black 5 (RB5) was obtained from a textile dyeing industry in Thailand. The chemical structures of RB5 is illustrated in Fig. 1. Commercial zerovalent iron and silver (purity 99%) were purchased from SD Fine Chem Limited (particle size 100 mesh). Ferrous chloride (($FeCl_2{\cdot}6H_2O$), ferric chloride ($FeCl_3{\cdot}6H_2O$), and silver chloride (AgCl) were obtained from Ajax. Hydrochloric acid (HCl) was purchased from JT Baker. Sodium hydroxide (NaOH) was purchased from Carlo Erba Réactifs-SdS.

2.2. Experimental setup

The stock solution of 0.1 mM of RB5 was prepared by adding 991.82 mg of RB5 to 1 L deionized water (DI water). Batch experiments were conducted to examine the efficiency of PS activated by Fe^{2+} to decolorize RB5 in an aqueous solution. The initial RB5 concentration was 0.01 mM (100 mg L^{-1}). One hundred milliliters of aqueous RB5 was treated with a ratio of 200 mM PS to 1 mM Fe^{2+}, 200 mM PS, or 1 mM Fe^{2+} in 250-mL Erlenmeyer flasks. The flasks were covered with Parafilm (American National Can, Chicago, IL) and agitated on an orbital shaker at 150 rpm at ambient temperature. The experiment was performed for 48 h. At preselected times, the samples were collected.

2.3. Effects of PS dosage, activator dosage, and initial concentrations of RB5

The RB5 solutions were treated by four different concentrations of PS (200, 300, 400, and 500 mM) with 1 mM Fe^{2+} as the activator. In addition, the RB5 solutions were treated by 400 mM PS with four different concentrations of Fe^{2+} (0.5, 1, 4, and 8). In the final batch, the RB5 solutions were prepared in deionized water at five initial concentrations of 0.01, 0.02, 0.03, 0.04, and 0.05. One hundred milliliters of dye solution was poured into a 250-mL Erlenmeyer flask and treated by 400 mM PS and 4 mM Fe^{2+}. All flasks were shaken by a rotating shaker at 150 rpm. The experiment was performed in triplicate and conducted at room temperature. At preselected times, the samples were collected.

2.4. Effect of pH, types of activator, and NaCl

We used a pH-stat apparatus (Metrohm Titrino 718S; Brinkman Instruments, Westbury, NY) to control the pH in the PS-Fe^{2+}-reactive dye matrix. A single treatment, consisting of 0.01 mM of RB5, 400 mM PS, and 4 mM Fe^{2+} was used in this study. The treatments were held at pH 5, 7, 9, and 11. An acidic pH was obtained by adding 0.1 N HNO_3, while a basic pH was obtained by adding 0.2 N NaOH. Changes in the RB5 concentrations were measured at preselected times over a 12 h period. The experiment was performed in triplicate and conducted at room temperature. A batch experiment was performed to investigate the effects of activator types on the decolorization of RB5. Five activators (Fe^0, Fe^{2+}, Fe^{3+}, Ag^0, and Ag^+) were chosen in this study. The initial RB5 concentration was 0.01 mM (100 mgL^{-1}). One hundred milliliters of aqueous RB5 was treated with a ratio of 400 mM PS to 4 mM of each activator in 250-mL Erlenmeyer flasks. The 0.01 mM RB5 solutions were treated with 400 mM PS, 4 mM Fe^{2+}, and four different concentrations of NaCl (17.24 mM (1gL^{-1}), 34.48, 51.72, and 68.96). All flasks were shaken by a rotating shaker at 150 rpm. Both experiments were performed in triplicate and conducted at room temperature. At preselected times, the samples were collected.

2.5. Chemical analysis

The samples were collected by filtration through a 0.45-μm membrane filter. The residual concentration of RB5 was quantified by a UV/VIS 918 spectrophotometer at 598 nm. The intermediates of RB5 reduction by PS oxidation were analyzed by 6490 Triple Quadrupole LC-MS Systems. The column used for

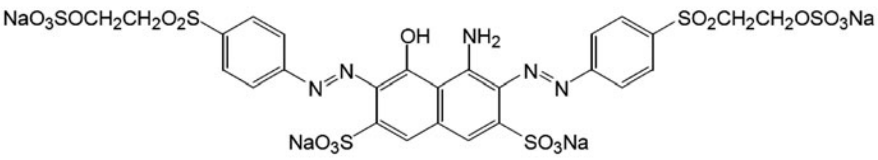

Fig. 1. Molecular structure of RB5.

LC-MS analysis was Zorbax SB-C18 (2.1 × 150 mm). The flow rate for this procedure was 0.20 mL min^{-1} with a repeated injection volume of 5 µL. A mobile phase of methanol (in H_2O mixed with 0.05% formic acid) was used with the following gradient: 5:95 (MeOH:H_2O) for 10 min followed by 10:90 for 5 min and 100:0 for the remainder of the run (~30 min). The UV detector was used at 254 nm for RB5 degradation products. Mass spectra were obtained using an ion—trap mass spectrometer fitted with an electron spray interface operated in positive ionization mode with a spray voltage of 3.5 kV, at a capillary temperature of 200˚C. Mineralization of the RB5 solutions during PS oxidation was followed by measuring the total organic carbon (TOC) using TOC analyzer, Tekmar Dohrmann, Phoenix 8000. The samples were introduced into the combustion furnace operated at 700˚C on platinum-based catalyst. The CO_2 generated was swept by oxygen through a non-dispersive infrared detector.

2.6. Response surface methodology

RSM was used to investigate the influence of the PS dosage, activator dosage, and pH on the decolorization of 0.01 mM RB5. The central composite design (CCD) method was chosen to evaluate the combination effects on three factors namely, the PS dosage (X_1), the activator dosage, (X_2), and the pH (X_3). The CCD required an experiment number according to $N = K^2 + 2K + c_p$ where k is the factor number and c_p is the replicate number of the central point. All factors were studied in five levels (–α, –1, 0, +1, and +α) according to $\alpha = 2^{k/4}$where k is the factor number [32]. This experimental design was performed using five level values: maximum (+1.68), +1, 0, –1, and minimum (–1.68). The level and code for each factor and the design for the RSM are shown for the actual values in Table 1 and for the predicted values in Table 2.

Khuri and Cornell [33] described an empirical second-order polynomial model for three factors using RSM by Eq. (3):

$$Y = \beta 0 + \sum \beta iXi + \sum \beta ijXiXj + \sum \beta ijXi^2 \tag{3}$$

where Y is the predicted response (% removal efficiency of RB5 by PS oxidation) and β is the model coefficient parameter. The removal efficiency was calculated using Eq. (4):

$$Y\ (\%) = \frac{C_0 - C}{C_0} \times 100 \tag{4}$$

Table 1
Level and code of factors for RSM

Factors	Codes	Level				
		−1.682	−1	0	1	1.682
PS (mM)	X_1	232	300	400	500	568
Fe^{2+} (mM)	X_2	0.64	2	4	6	7.36
pH	X_3	2.64	4	6	8	9.36

where C_0 is the initial concentration of RB5 and C is the concentration of RB5 after treating with PS and Fe^{2+} at 4 h. The results were analyzed with statistical software.

3. Results and discussion

3.1. Decolorization of RB5 by PS oxidation

We determined the efficiencies of using 200 mM PS activated by 1 mM Fe^{2+}, 200 mM PS alone, or 1 mM Fe^{2+} to degrade 0.01 mM of RB5 in aqueous solutions. The initial pH of RB5 solution was 7.78 ± 0.25. The reductions of RB5 are illustrated in Fig. 2(A). In Fig. 2(A), the Fe^{2+} alone had no significant effects on decolorization of RB5. In treatment of RB5 with PS alone, the decolorization began to slow down at 6 h, reached a plateau at 12 h, and remained at this concentration until the end of the experiment. The decolorization in the treatment of RB5 with PS/Fe^{2+} started slowing down at 10 h, reached a plateau at 14 h, and the RB5 color was completely gone. The decolorization of RB5 by PS oxidation with and without Fe^{2+} seemed to follow a pseudo-first-order kinetic and the degradation curve was fit with the exponential decay equation. The pseudo-first-order decolorization rate (k_{obs}) of RB5 by PS oxidation was calculated using Eq. (5):

$$-\frac{d[\text{RB5}]}{dt} = k_{\text{obs}}[\text{RB5}] \tag{5}$$

where [RB5] is the concentration of RB5, t is time, and the k_{obs} value is 0.2265 h^{-1} for RB5 treatment by 200 mM PS activated by 1 mM Fe^{2+}, whereas k_{obs} value is 0.0218 h^{-1} for RB5 treatment by 200 mM PS alone. Treating RB5 by PS alone provided less efficiency than using PS activated by Fe^{2+}. In the PS/Fe^{2+}/RB5 system, the possible decolorization reaction could be expressed by Eqs. (6)–(10):

$$S_2O_8^{2-} + Fe^{2+} \rightarrow Fe^{3+} + SO_4^{2-} + SO_4^{-\cdot} \tag{6}$$

Table 2
The experimental design for RSM and % removal efficiency

Trial #	Factor level X_1	X_2	X_3	Actual values X_1	X_2	X_3	% RB5 decolorization Experimental	Predicted
1	−1	−1	−1	300	2	4	50.23	45.97
2	−1	−1	+1	300	2	8	56.25	53.53
3	−1	+1	−1	300	6	4	60.25	65.65
4	−1	+1	+1	300	6	8	50.12	53.05
5	+1	−1	−1	500	2	4	60.21	59.57
6	+1	−1	+1	500	2	8	68.25	65.13
7	+1	+1	−1	500	6	4	85.42	90.45
8	+1	+1	+1	500	6	8	69.24	75.85
9	−1.682	0	0	232	4	6	43.25	45.40
10	0	−1.682	0	400	0.64	6	40.23	48.25
11	0	0	−1.682	400	4	2.64	78.52	77.19
12	+1.682	0	0	568	4	6	80.14	75.97
13	0	+1.682	0	400	7.36	6	83.24	73.79
14	0	0	+1.682	400	4	9.36	71.42	71.27
15	0	0	0	400	4	6	97.26	91.73
16	0	0	0	400	4	6	87.25	91.73
17	0	0	0	400	4	6	91.24	91.73
18	0	0	0	400	4	6	93.25	91.73
19	0	0	0	400	4	6	93.14	91.73
20	0	0	0	400	4	6	85.26	91.73

$$SO_4^{-\bullet} + H_2O \rightarrow SO_4^{2-} + H^+ + {}^{\bullet}OH \text{ (hydroxyl radical)} \tag{7}$$

$$SO_4^{-\bullet} + RB5 \rightarrow SO_4^{2-} + RB5\,\text{intermediate} \tag{8}$$

$${}^{\bullet}OH + RB5 \rightarrow OH^- + RB5\,\text{intermediate} \tag{9}$$

$$SO_4^{-\bullet} + {}^{\bullet}OH + RB5\,\text{intermediate} \rightarrow SO_4^{2-} + CO_2 + H_2O + \text{other inorganics} \tag{10}$$

Sulfate radicals might dominate the reaction of the decolorization of RB5 although other oxidizing species could exist in the system [34]. Mineralization of 0.01 mM RB5 solution during PS oxidation (Eq. (10)) was followed by measuring TOC content of the samples. Fig. 2(B) shows the decrease of TOC vs. time for decolorization of RB5 by PS oxidation. The Fe^{2+} alone had no significant effects on mineralization of RB5. We found a few mineralization on RB5 treated by PS alone. The major mineralization was obtained with PS oxidation activated by Fe^{2+}. Although the RB5 decolorization with the PS/Fe^{2+} occurred quickly within 8 h, the reduction of TOC was more slowly than the RB5 decolorization. At 12 h, the color of RB5 was completely gone (100% decolorization) while TOC reduction had still proceeded until 24 h. The TOC removal efficiency was only 70%. If the oxidation was completed, the final products should be CO_2, H_2O, SO_4^{2-}, and NO_3^-. However, this indicated that there were some organic intermediates remaining in the treatment. Some researchers observed similar results for the oxidation process of dye; the organic materials were not completely mineralized because stable intermediates were formed, for example, acetic acid [35,36].

In addition, the rate of TOC removals was positively related to the PS concentration in the range of 1–4 mM. The excessive PS would complete with sulfate radicals through reaction in Eq. (11) [19,34]:

$$SO_4^{-\bullet} + S_2O_8^{2-} \rightarrow S_2O_8^{2-} + 2SO_4^{2-} \tag{11}$$

The UV spectra of wastewater containing RB5 before and after treating with 200 mM PS activated by 1 mM Fe^{2+} are shown in Fig. 3. It seems that the main spectrum of light absorption of RB5 before the treatment was located at 598 nm and the second spectrum was located at 328 nm. The peak at 328 nm was assigned to its aromatic rings while the peak at 598 nm was assigned to the conjugated structure formed by the azo bond of RB5 [37,38]. As the chemical oxidation proceeded, the absorption peak at 598 and 328 nm decreased dramatically and disappeared within 24 h,

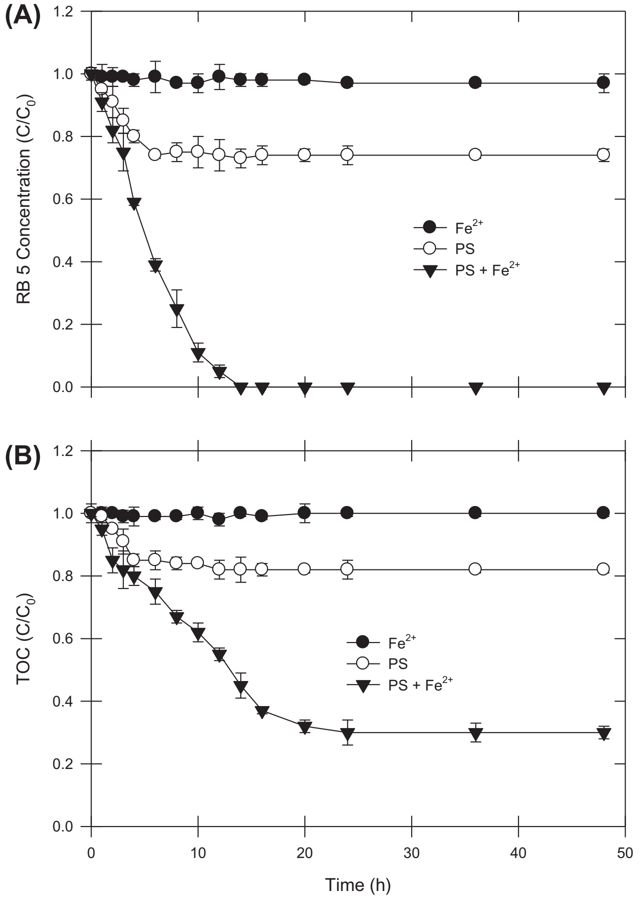

Fig. 2. Decolorization (A) and mineralization (B) of RB5 by 200 mM PS activated by 1 mM Fe^{2+}, 200 mM PS alone, and 1 mM Fe^{2+} alone.

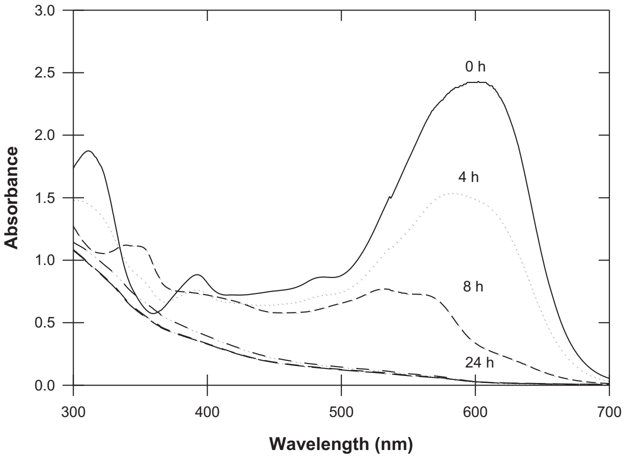

Fig. 3. UV spectrum of degradation of RB5 by 200 mM PS activated by 1 mM Fe^{2+}.

which indicated that the chromophore was completely destroyed. Loukanov et al. [38] reported that the oxidation processes of RB5 occurred not only in the azo group, but also there was destroying the aromatic structure. The intermediates, naphthionic acid, 1-amino-2-naphtol, 2-naphtol, and 1,2-naphthoquinone were found in photolysis of RB5 [39]. The azo dyes contain one or more azo groups –N=N–, as the chromophore, which is the basic functional group for visible color in dyes. The molecular structure of RB5 has two azo groups. In the chemical structure of RB5, 1-sulfonic, 2-(benzenesulfonyl) ethanol connects to an azo bond (Fig. 1). Initially, the sulfate radicals/hydroxyl radicals oxidized the azo group and opened the –N=N–. The decolorization of RB5 proceeded via reductive cleavage of azo bonds resulting in the formation of amines and naphthalene. To confirm the reductive cleavage of azo bonds, a sample at 4 h was examined by LC-MS analysis. The mass spectra (Fig. 4) indicated that 2,7,8-triaminonaphthalen-1-ol or 4-(ethylsulfonyl) benzenamine, with an *m*/*z* ratio of 189, might possibly result from the –N=N– cleavage in the molecular structure as one of the decolorization products of RB5 decolorization by PS. Our results confirmed that the disappearances of RB5 occurred when the chromophores had broken down. Yu et al. [6] observed similar results for the decolorization of RB5 in a UV/TiO_2 system. During the decolorization, hydroxyl radicals (OH·) generating in the system attacked the azo bond and then –N=N– linkages were destroyed. Kritikos et al. [40] also showed that the products of the photocatalytic decolorization of RB5 were aromatic rings and short-chain aliphatic oxygenated hydrocarbons.

3.2. Effects of PS dosage and activator dosage

We determined the efficiency of using 200, 300, 400, and 500 mM of PS with a fixed concentration of Fe^{2+} (1 mM) to treat 0.01 mM RB5. The decolorization of RB5 by different PS dosages is illustrated in Fig. 5(A). When the PS dosage increased from 200 to 400 mM, the k_{obs} value of the RB5 decolorization increased. The k_{obs} values of the RB5 decolorization by 200, 300, 400, and 500 mM of PS were 0.2343, 0.2687, 0.5686, and 0.5777 h^{-1}, respectively. The removal efficiencies of RB5 by 200, 300, 400, and 500 mM of PS with 1 mM Fe^{2+} at 4 h were 67 ± 0.02%, 79 ± 0.05%, 94 ± 0.01%, and 94 ± 0.05%, respectively. However, a further increase in the PS dosage resulted in a slight increase in the k_{obs}. The same trend was found for the decolorization of the azo dye Orange G by PS with the ferrous ion [37]. Liang et al. [41] indicated that the influence of persulfate on the oxidation of BTEX under a fixed Fe^{2+} concentration was less significant. The

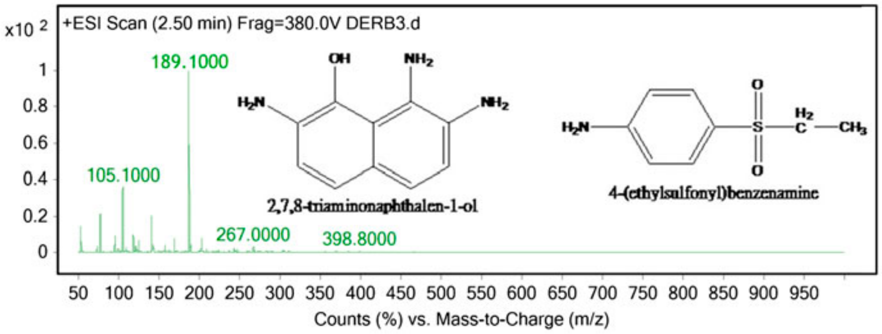

Fig. 4. Mass spectrum of intermediates of RB5 treated by PS/Fe^{2+} at 4 h.

plot of k_{obs} vs. the concentration of PS is presented in Fig. 5(B). It seemed that the k_{obs} and PS were not significantly related by either a linear or a non-linear relationship. The suitable condition in this experiment was the use of 400 mM of PS; therefore, in the subsequent experiment, 400 mM PS was used to study the effects of the activator dosage.

The oxidation of RB5 by 400 mM with different Fe^{2+} concentrations is shown in Fig. 5(C). The decolorization of RB5 increased as the activator dosage increased. The k_{obs} values of the RB5 decolorization by 400 mM of PS activated with 0.5, 1, 4, and 8 mM Fe^{2+} were 0.1019, 0.5745, 1.1846, and 2.0296 h^{-1}, respectively. The removal efficiencies of RB5 by 400 mM of

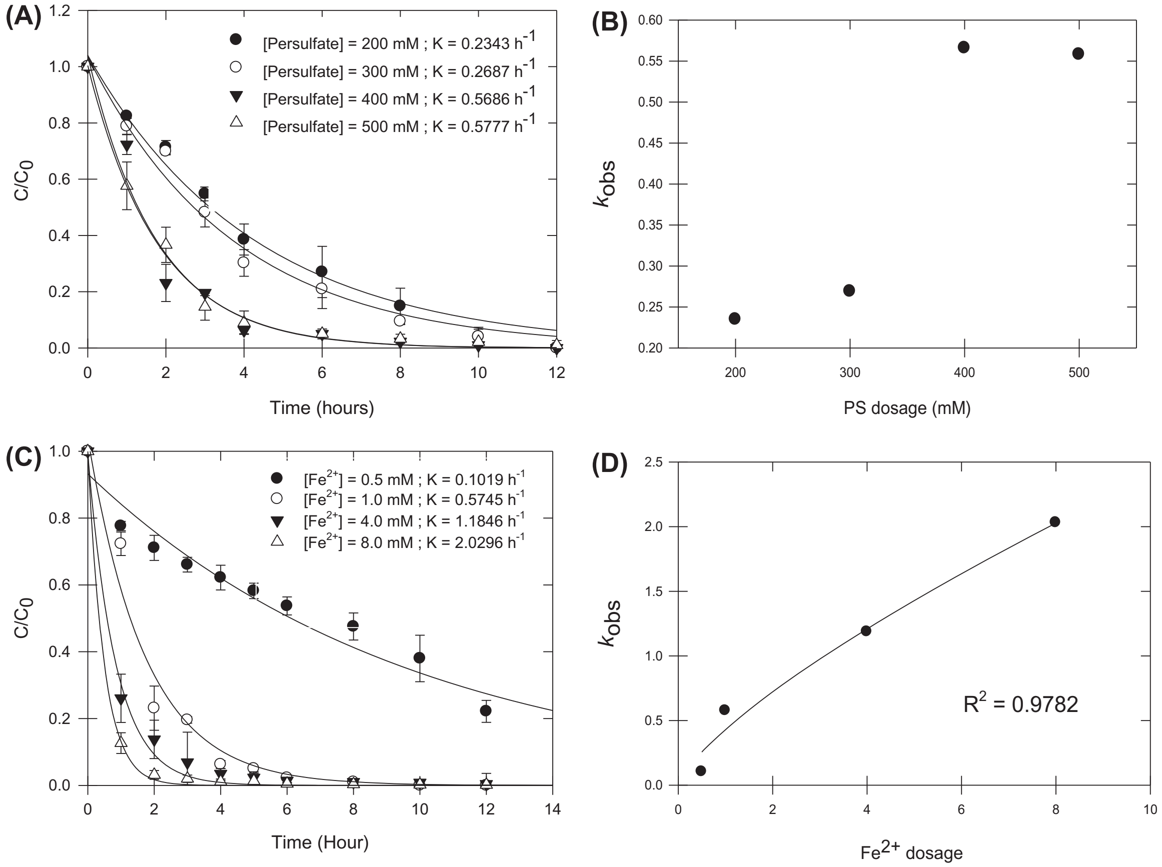

Fig. 5. The decolorization of RB5 by different PS concentrations (A), the plot of k_{obs} vs. the concentration of PS (B), the decolorization of RB5 by different activator (Fe^{2+}) dosages (C), and the plot of k_{obs} vs. the concentrations of activator (D).

PS activated with 0.5, 1, 4, and 8 mM Fe^{2+} at 4 h were 46 ± 0.08%, 77 ± 0.01%, 96 ± 0.09%, and 98 ± 0.01%, respectively. Higher decolorization efficiencies were achieved with higher initial Fe^{2+} concentrations which were chiefly attributed to the increased generation of $SO_4^{-\cdot}$ [42]. Similar results have been reported in other studies [37,43]. The comparison of the k_{obs} values may be inaccurate due to a possible non-linear relationship between the k_{obs} and the Fe^{2+} loading. The plot of the k_{obs} vs. the concentration of Fe^{2+} is presented in Fig. 5(D). The increase in the concentration of Fe^{2+} enhanced the generation of sulfate radicals and hence, the k_{obs} value increased. The non-linear relationship between the Fe^{2+} dosage and Fe^{2+} is given by $K_{obs} = 0.43[Fe^{2+}]^{0.74}$ with $R^2 = 0.9782$. A similar trend in the kinetic model had been observed for the reduction of Alizarin Red S by ammonium persulfate using Fe^0 as the catalyst [21].

On the other hand, overloading of the activator may hinder the decolorization efficiency of RB5. Fe^{2+} could also act as a scavenger of $SO_4^{-\cdot}$, effectively quenching the oxidation reaction in Eq. (12) [42]:

$$Fe^{2+} + SO_4^{-\cdot} \rightarrow Fe^{3+} + SO_4^{2-} \tag{12}$$

Moreover, the excess of $SO_4^{-\cdot}$ generated by Fe^{2+} may be consumed by some reactions other than with RB5. The possible reactions are shown in Eqs. (13)–(18) [37]:

$$SO_4^{-\cdot} + SO_4^{-\cdot} \rightarrow 2SO_4^{2-} \tag{13}$$

$$SO_4^{-\cdot} + H_2O \rightarrow HSO_4^- + {}^{\cdot}OH \tag{14}$$

$$SO_4^{-\cdot} + {}^{\cdot}OH \rightarrow HSO_4^- + 1/2\ O_2 \tag{15}$$

$${}^{\cdot}OH + {}^{\cdot}OH \rightarrow H_2O_2 \tag{16}$$

$$SO_4^{-\cdot} + H_2O_2 \rightarrow SO_4^{2-} + H^+ + HO_2\cdot \tag{17}$$

$$SO_4^{-\cdot} + HO_2^{\cdot} \rightarrow SO_4^{2-} + H^+ + O_2 \tag{18}$$

3.3. Effects of initial concentration of RB5

The effect of the initial concentration of RB5 on the decolorization by PS was investigated. The initial concentrations of RB between 0.01 and 0.05 mM were treated by 400 mM PS activated by 4 mM Fe^{2+}. The effect of initial concentration of RB5 is shown in Fig. 6(A). The higher initial concentration of RB5, the lower decolorization efficiency. The k_{obs} values of the RB5 decolorization at initial concentrations of 0.01, 0.02, 0.03, 0.04, and 0.05 mM by 400 mM of PS activated with 4 mM Fe^{2+} were 0.482, 0.2339, 0.1296, 0.0918, and 0.0817 h^{-1}, respectively. The removal efficiencies of 0.01, 0.02, 0.03, 0.04, and 0.05 mM RB5 by 400 mM of PS activated with 4 mM Fe^{2+} at 4 h were 82 ± 0.08%, 60 ± 0.04%, 43 ± 0.02%, 38 ± 0.02%, and 28 ± 0.02%, respectively. The relationship between k_{obs} and the initial concentration of RB5 is shown in Fig. 6(B). The relationship is non-linear and the best fit was achieved with an exponential function with $R^2 = 0.9918$: $K_{obs} = 0.665e^{-50.46[RB5]}$ where [RB5] is the initial concentration of RB5. A similar trend in the kinetic model had been observed for the reduction of Alizarin Red S by ammonium persulfate using Fe^0 as the catalyst [21]. In fact, as the RB5 concentration increased, the number of sulfate radicals did not increase proportionally.

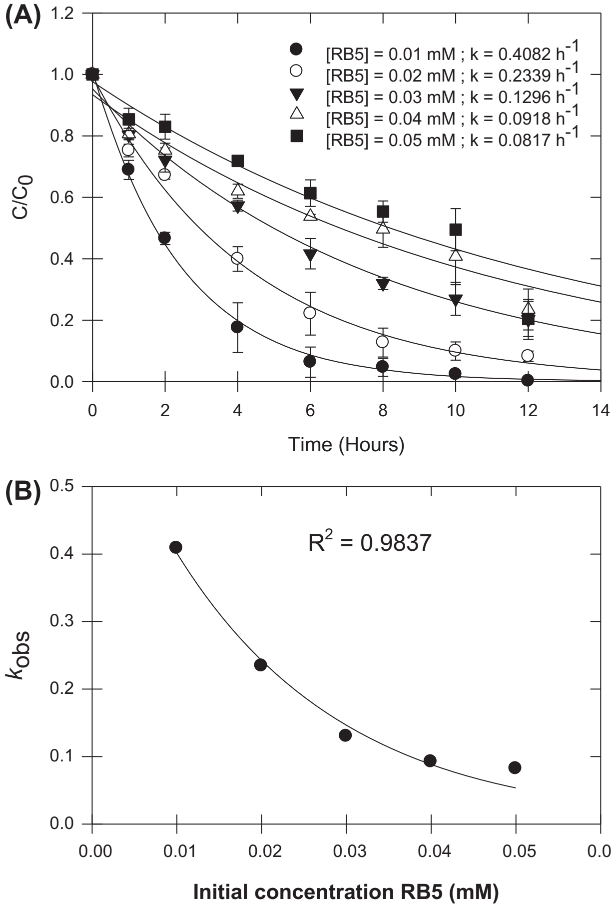

Fig. 6. The decolorization of RB5 at different initial concentrations by 400 mM PS and 4 mM Fe^{2+} (A) and the plot of k_{obs} vs. the initial concentrations of RB5 (B).

3.4. Effect of pH

To study the effect of pH, a pH-stat was used to control the pH of an aqueous solution of RB5. The RB5 solutions were treated by 400 mM PS and 4 mM Fe^{2+} at four different pH levels (5, 7, 9, and 11). The decolorization of RB5 by 400 mM and 4 mM Fe^{2+} at different pH levels is shown in Fig. 7(A). The decolorization of RB5 decreased when the pH increased. The k_{obs} values of the RB5 decolorization by 400 mM of PS and 4 mM Fe^{2+} at pH levels of 5, 7, 9, and 11 were 0.499, 1.1075, 1.6486, and 2.5472 h^{-1}, respectively. The removal efficiencies of RB5 by 400 mM of PS and 4 mM Fe^{2+} at pH levels of 5, 7, 9, and 11 at 4 h were 99 ± 0.01%, 96 ± 0.04%, 94 ± 0.08%, and 75 ± 0.17%, respectively. With the increase of pH from 5 to 10, the decolorization of RB5 by PS decreased, which indicated that an acidic pH is more favorable to the reaction of PS with regard to the oxidation of RB5. At a higher pH, the concentration of Fe^{2+} could decrease due to the formation of Fe^{2+} complexes which hinder the further reaction of Fe^{2+} with PS. The iron oxides formed in the treatment system, such as, $FeOH^{2+}$, $Fe_2(OH)_2{}^{4+}$, $Fe(OH)_2{}^{+}$, $Fe(OH)_3$, and $Fe(OH)_4{}^{+}$ have low efficiency in the activation of persulfate to produce the sulfate radicals [34]. In addition, at high pH (e.g. pH > 8.5), the substantial concentration of PS present in the solution may scavenge the ·OH formed upon reaction of the former with hydroxyl anions that are favored in alkaline solution as shown in Eq. (19) [23]. This might result in the rapid decay of sulfate radicals.

$$SO_4^{-}\cdot + OH^{-} \rightarrow SO_4^{2-} + {}^{\cdot}OH \tag{19}$$

Another possible way was for the carbon dioxide formed from the RB5 mineralization in Eq. (10) to lead to the formation of bicarbonate (HCO_3^-) and carbonate (CO_3^{2-}) ions under alkaline conditions which might inhibit the RB5 decolorization [34,44]. Zuo and Katsumura [45] indicated that at a high pH, $SO_4^{-}\cdot$ could react with HCO_3^- and CO_3^{2-} as Eqs. (20) and (21) resulting in sulfate radicals in the system being consumed.

$$SO_4^{-}\cdot + HCO_3^{-} \rightarrow SO_4^{2-} + HCO_3^{\cdot} \text{ at pH } 8.4 \tag{20}$$

$$SO_4^{-}\cdot + CO_3^{2-} \rightarrow SO_4^{2-} + CO_3^{-}\cdot \text{ at pH} > 8.4 \tag{21}$$

Yang et al. [3] also reported that carbonate could activate peroxymonosulfate to generate $SO_4^{-}\cdot$ which rapidly reacted with OH^- to produce OH·, even at a low concentration, and it could quench OH· and inhibit the decolorization of the azo dye Acid Orange 7.

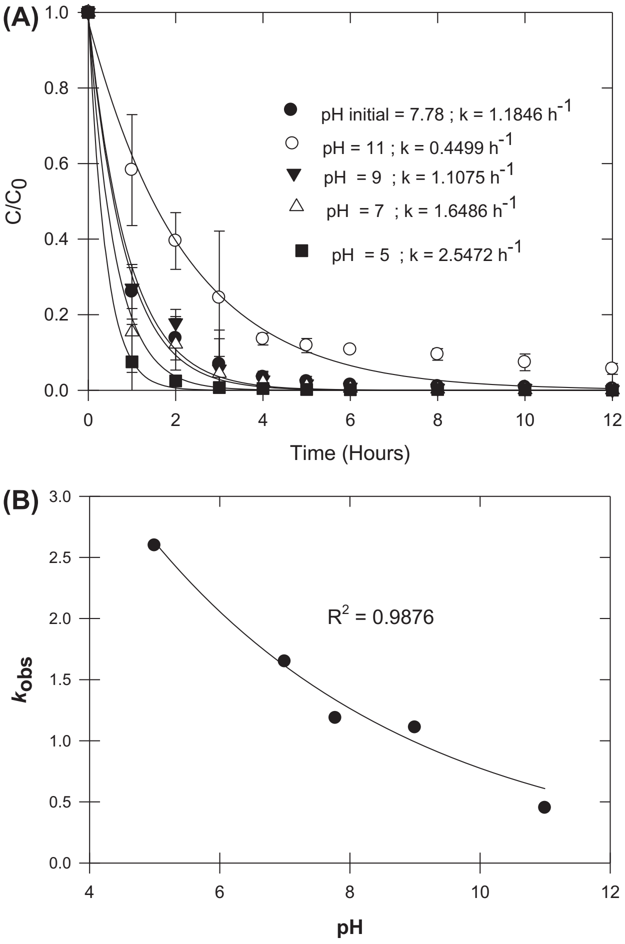

Fig. 7. The decolorization of RB5 at different pHs by 400 mM PS and 4 mM Fe^{2+} (A) and the plot of k_{obs} vs. pHs (B).

The plot of the k_{obs} vs. the concentration of Fe^{2+} is presented in Fig. 7(B). The relationship shown is nonlinear and the best fit was by an exponential function with $R^2 = 0.9876$—namely, $K_{obs} = 8.871e^{-0.2477[\text{pH}]}$ Similar trends have been observed for the reduction of Methylene Blue [23] and Orange G [37].

3.5. Types of activator

Five activators (Fe^0, Fe^{2+}, Fe^{3+}, Ag^0, and Ag^+) were chosen to study their capability in activating PS oxidation. The decolorization of 0.01 mM RB5 treated by 400 mM PS with 4 mM of the five different activators is presented in Fig. 8. The k_{obs} values of the RB5 decolorization by 400 mM of PS and 4 mM of Fe^0, Fe^{2+}, Fe^{3+}, Ag^0, and Ag^+ were 2.8609, 1.2772, 1.1846, 0.5639, and 0.2499 h^{-1}, respectively. The removal efficiency at 2 h of RB5 treated by 400 mM of PS and 4 mM of Fe^0, Fe^{2+}, Fe^{3+}, Ag^0, and Ag^+ was 100%, 94 ± 0.02%, 91 ± 0.07%, 55 ± 0.04%, and 37 ± 0.06%, respectively. At the equivalent mole of activator, the k_{obs} of the treatment by PS activated by Fe^0 produced the best kinetic rate. Fe^0 might serve as a slow-releasing source of dissolved Fe^{2+}, which would activate PS to produce $SO_4^{-\bullet}$ as described in Eqs. (22) and (23) [42], while PS activated by Fe^{2+} may be limited by the $SO_4^{-\bullet}$ scavenging due to excessive iron according to Eqs. (23) and (24) [46]:

$$Fe^0 + S_2O_8^{2-} \rightarrow Fe^{2+}\ 2SO_4^{2-} \tag{22}$$

$$Fe^{2+} + S_2O_8^{2-} \rightarrow Fe^{3+} + SO_4^{-\bullet} + SO_4^{2-} \tag{23}$$

$$Fe^{2+} + SO_4^{-\bullet} \rightarrow Fe^{3+} + SO_4^{2-} \tag{24}$$

Another possible process would involve the Fe^0 being able to activate PS by involving a direct electron transfer from Fe^0 or surface bound Fe^{2+} (i.e. Fe^{2+} adsorbed to the iron surface or to structural Fe^{2+} in the form of an iron oxide) [42].

In dye treatment, previous research has shown that Fe^0 itself can successfully transform many dyes, such as Orange I, Orange II, Crocein Orange G, Sunset Yellow FCF [47], and diazo dye CI Acid Black 24 [48], Acid Orange 2 [49], Reactive Red 2 [50], and Reactive Black 5 [51]. In dye decolorization, the azo bond (N=N) of the chromophore or chromogen of the dye is broken by an electron provided by Fe^0, and the color disappears. Feng et al. [50] used the GC/MS technique to investigate the degradation products of Reactive Red 2 by Fe^0. Their results confirmed that the azo linkage of Reactive Red 2 was reduced to a hydrogenated azo structure without the destruction of the benzene or naphthalene rings. However, the disadvantage of using Fe^0 as a activator is that Fe^0 may generate the excessive Fe^{2+} in the system leading to produce a lot of iron oxides after treatment.

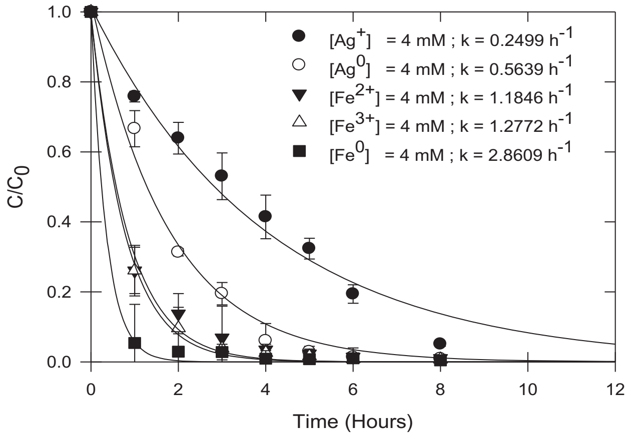

Fig. 8. The decolorization of RB5 by 400 mM PS and 4 mM of Fe^0, Fe^{2+}, Fe^{3+}, Ag^0, and Ag^+.

It was found that adding Fe^{2+} or Fe^{3+} without PS did not show any decolorization of RB5. However, Fe^{2+} or Fe^{3+} ions could significantly accelerate the oxidation of RB5 in the presence of PS. Compared with the Fe species, the Ag species (Ag^0 and Ag^+) were less effective as activators for the RB decolorization by PS. However, Anipsitakis and Dionysiou [19] reported that Ag^+ was the most efficient metal ion for the activation of PS under UV light among nine tested transition metals, but Ag^+ was not sufficient to activate PS in the dark.

3.6. Effects of NaCl

In the dyeing process, NaCl is commonly added to obtain a specific gravity which depends on the type of dye; consequently, a large amount of NaCl is released in the wastewater from textile dyeing mills. We determined the efficiency of using 400 mM of PS with 4 mM Fe^{2+} to treat 0.01 mM RB5 with various concentrations of NaCl: 17.24 mM (1 g L^{-1}), 34.48, 51.72, and 68.96. The effect of NaCl on the decolorization of RB5 by PS is shown in Fig. 9. The higher the concentration of NaCl, the lower the k_{obs} of the RB5 decolorization by PS. The k_{obs} values of the RB decolorization by PS under 17.24 mM (1 g L^{-1}), 34.48, 51.72, and 68.96 NaCl were 0.3132, 0.2360, 0.2129, and 0.1972 h^{-1}, respectively, while the k_{obs} value of the control treatment (without NaCl) was 1.1846 h^{-1}. The removal efficiencies at 4 h of treatment with NaCl were between 45 and 57% while the removal efficiency of the control increased to 93%. The same trend was found with the decolorization of the azo dye Orange G (OG) by PS with the ferrous ion [37]. Chloride may increase the ionic strength of the medium and thus, may affect the catalytic activity in physicochemical wastewater treatment [6]. In the presence of Cl^-, $SO_4^{\bullet-}$ can react with Cl^- as shown in Eq. (25), which would lead to a decrease in the amount of $SO_4^{-\bullet}$ in the treatment system [52]:

$$SO_4^{-\bullet} + Cl^- \rightarrow SO_4^{2-} + Cl^- \tag{25}$$

Liang et al. [53] reported that when the concentration of chloride exceeded 0.2 M, the TCE degradation by PS was inhibited due to a possible sink of sulfate radicals. In addition, if the chloride ions are present at an elevated concentration, the forward reaction of

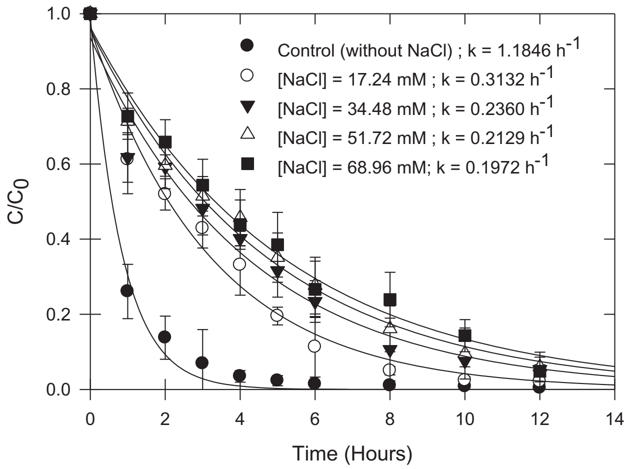

Fig. 9. The decolorization of RB5 in different NaCl concentrations by 400 mM PS and 4 mM of Fe^{2+}.

Eq. (23) would be important compared with the reverse reaction and would result in a greater degree of scavenging of $SO_4^{\cdot-}$. It was found that several anions may scavenge sulfate radicals and inhibit the reaction. Xu and Li [37] indicated that the anions could inhibit the reaction rate of OG decolorization and their inhibiting effects could be ranked from low to high in the order of $NO_3^- < Cl^- < H_2PO_4^{-\cdot} < HCO_3^-$. Prior to the application of PS, the wastewater should be screened for the presence of $SO_4^{-\cdot}$ scavengers to evaluate the removal efficiency of the treatment.

3.7. Analysis of RSM

The relationship between the three factors (PS dosage, activator dosage, and pH) and the decolorization efficiency of 0.01 mM RB5 was analyzed using RSM. The predicted response (Y) was assessed as a function of the PS dosage (X_1), the activator dosage (X_2), and the pH (X_3). Table 3 shows the statistical analysis of the model (ANOVA) for response surface quadratic model for RB5 removal by PS. The model F value is 15.21 and the value of "Prob > F" of the model is 0.0001. This implies that the inclusion of the three variables produced a statistically significant result, "Prob > F" is less than the 0.05 test level for significance used. The lack of fit (LOF) F-value is 3.32 and the value of "Prob > F" of LOF is 0.1070. The LOF of the model implied the variation of data around the fitted model. There is only a 10.70% chance that a "LOF F-value" this large could occur due to noise. The value of "Prob > F" of LOF higher than 0.05 shows that the F-statistic was insignificant, implying significant model correlation between the variable and process response [54]. The R^2 value gives the proportion of the total variation in the response predicted by the model indicating the ratio of the sum of squares due to the regression to the total sum of squares [29]. The R^2 value in this study was 0.9319 for the RB5 decolorization by PS while the adjusted R^2 was 0.8707. The R^2 value should be at least 0.80 for a good fit of a model [55]. A high R^2 value (close to 1) is desirable and reasonable agreement with the adjusted R^2 is necessary [56]. The predicted R^2 was 0.587 and the adequate precision was 10.248. The adequate precision measures signal to noise ratio. A ratio greater than 4 is desirable. Our ratio indicates the adequate signal, so the model can be used to navigate the design space. The relationship between the response and the three factors is expressed by the Eq. (26).

Table 3
ANOVA for response surface quadratic model for RB5 removal by PS

Source of variation	Sum of squares	Degree of freedom	Mean squares	F value	p-value prob > F
Model	5652.35	9	628.04	15.21	0.0001
X_1	1205.36	1	1205.36	29.20	0.0003
X_2	767.68	1	767.68	18.60	0.0015
X_3	42.84	1	42.84	1.04	0.3323
X_1X_2	62.22	1	62.22	1.51	0.2477
X_1X_3	2.03	1	2.03	0.049	0.8290
X_2X_3	203.72	1	203.72	4.94	0.0506
X_1^2	1707.20	1	1707.20	41.36	<0.0001
X_2^2	1702.76	1	1702.76	41.25	<0.0001
X_3^2	551.84	1	551.84	13.37	0.0044
Residual	412.79	10	41.28		
Lack of fit	317.22	5	63.44	3.32	0.1070
Pure error	95.57	5	19.11		
Cor. total	6065.14	19			

Note: $R^2 = 0.9319$; Adjusted $R^2 = 0.8707$; Predicted $R^2 = 0.5781$; Adequate precision = 10.248.

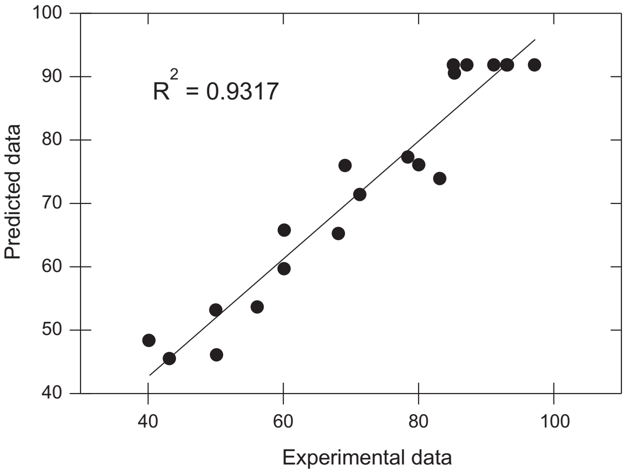

Fig. 10. The experimental data vs. predicted data plot for RB5 removal by PS.

$$Y = -243.75 + 0.93X_1 + 27.52X_2 + 23.76X_3 + 0.014X_1X_2 - 0.0025X_1X_3 - 1.26X_2X_3 - 0.0011X_1^2 - 2.72X_2^2 - 1.55X_3^2 \quad (26)$$

The predicted values calculated from the model and the experimental values are shown in Table 2. Fig. 10 shows the relationship between the predicted values and experimental values. The plot indicated an adequate agreement between real data and the ones obtained from the model. The experimental values are the measured response data for a particular run and the predicted values evaluated from the model and generated using approximating functions [57]. A diagnostic plot of the predicted vs. experimental values helps to determine whether the model is satisfactory [29]. Our result with $R^2 = 0.9317$ indicates an adequate agreement between the real data and the data obtained from the model.

The response surfaces for the RB5 decolorization efficiency are shown in Fig. 11. Each plot represents the effect of two variables in this study. The effects of the persulfate dosage and Fe^{2+} dosage, the persulfate dosage and pH, and the Fe^{2+} and pH are shown in Fig. 11(A)–(C), respectively. The shapes of all contour plots indicate the nature and extent of the interaction. Prominent interactions are shown by the elliptical nature of the contour plots, while less prominent or negligible interactions will be shown by the circular nature of the contour plots [27]. Our response plots and contour plots show clear peaks, indicating that the optimum conditions for maximum

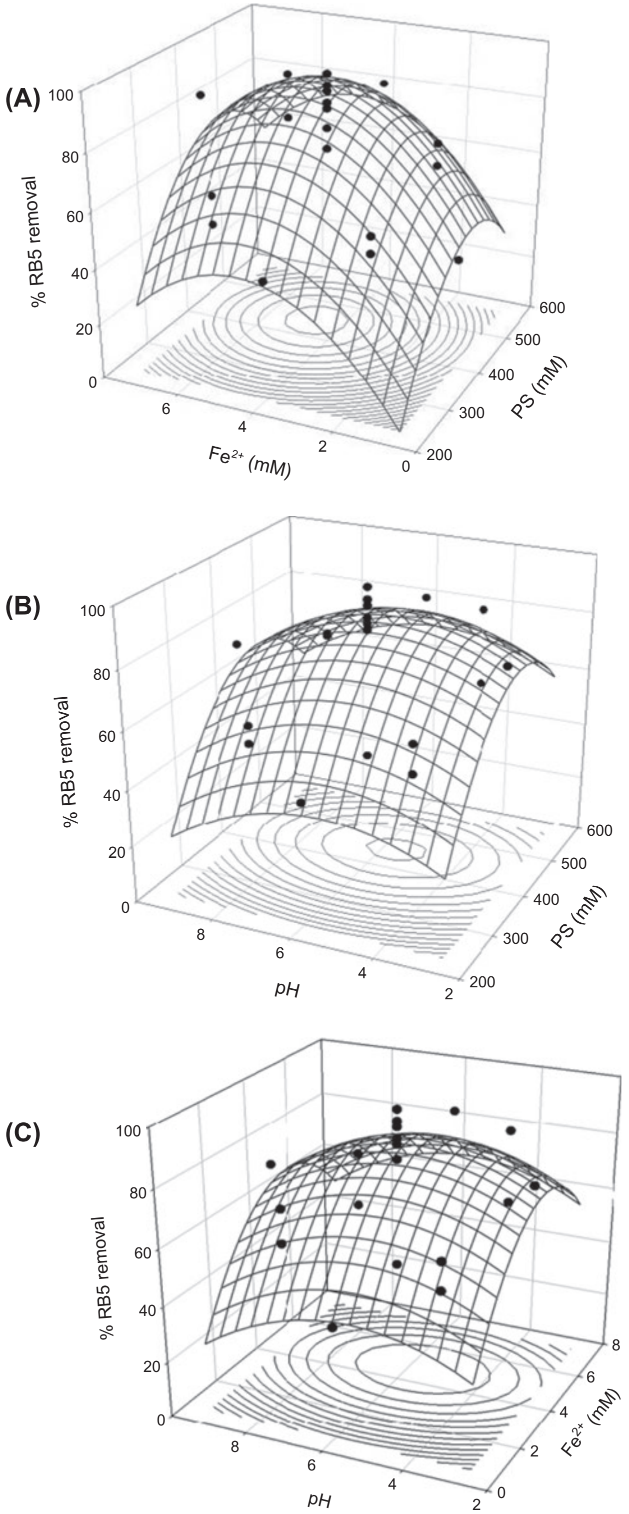

Fig. 11. Response surface plots showing the effects of PS dosages and Fe^{2+} dosages (A), PS dosages and pH (B), and Fe^{2+} dosages and pHs (C).

_values of the responses are attributed to the persulfate dosage, the Fe^{2+} dosage, and the pH, respectively. In Fig. 11(A), the optimal condition between PS dosage and Fe^{2+} dosage is obtained at 440 mM PS and 4.78 mM Fe^{2+}. The best condition between PS dosage and pH is 435 mM at pH 5.55 (Fig. 11(B)). The suitable condition between Fe^{2+} dosage and pH in Fig. 11(C) is 4.92 mM Fe^{2+} at pH 5.81. The overall optimum removal from the model was obtained at 445 mM PS and 4.91 mM Fe^{2+} at pH 5.45. The constraints of using these optimized values are that the concentration of RB5 must be less than 0.01 mM and the RB5 must not be contaminated by other chemicals for example, other dyes, salts, and heavy metals. In addition, the treatment must be done under room temperature. The experiments using the optimum condition were performed to confirm the model adequacy for determining the efficiency of RB5 removal. The results showed that the average RB5 removal efficiency at 4 h was 90.42% in the experiments while it was 96.08% in the model prediction. These results indicated that the RB5 removal efficiencies for all response parameters obtained from the experiments and the model predictions were in close agreement. The good agreement between the predicted and experimental results verified the validity of the model and reflected the existence of an optimal point [27].

4. Conclusion

The results of this study indicated that RB5 dye can be effectively degraded by persulfate oxidation using Fe^{2+} as the activator. It was found that the reaction of the RB5 decolorization by PS followed a pseudo-first-order kinetic model. The complete decolorization of RB5 by 200 mM PS activated by 1 mM Fe^{2+} was 100% within 12 h but the TOC removal efficiency was only 70% within 24 h. The decolorization of RB5 proceeded via reductive cleavage of azo bonds resulting in the formation of amines or naphthalenes. The mass spectra indicated that 2,7,8-triaminonaphthalen-1-ol or 4-(ethylsulfonyl) benzenamine with an *m*/*z* ratio of 189 that might result from N=N cleavage in the molecular structure was one of the degradation products of the RB5 decolorization by PS. When the PS dosage and Fe^{2+} dosage increased, the k_{obs} of the RB5 decolorization increased. When the RB5 concentration increased, the number of sulfate radicals did not increase proportionally, so the k_{obs} of the RB5 decolorization decreased. Lowering the pH from 11 to 5 increased the kinetic rates of destruction of RB5. Five activators (Fe^0, Fe^{2+}, Fe^{3+}, Ag^0, and Ag^+) were chosen to study their capability as activators in PS oxidation. At the equivalent mole of activator, the k_{obs} of the treatment of PS activated by Fe^0 was the best (2.8609 h^{-1}). Increasing the NaCl concentration from 17.24 mM (1 g L^{-1}) to 68.96 mM (4 g L^{-1}) decreased the kinetic removal rates of RB5. The RSM approach allowed the estimation of the influence of the three variables (persulfate dosage, Fe^{2+} dosage, and pH) on the RB5 decolorization by PS. The optimum removal from the model was obtained at 445 mM PS and 4.91 mM Fe^{2+} at pH 5.45. RSM is a good tool for determining the optimum conditions of PS treatment with a statistically reliable analysis.

Acknowledgment

This research was supported by the Kasetsart University Research and Development Institute (KU-RDI). We also thank Assistant Professor Dr Prapaipid Chairattanamanokorn for the RSM analysis and Dr Chatnat Chokejaroenrat for LC-MS analysis.

References

[1] S. Afaq, K.S. Rana, Toxicological effects of leather dyes on total leukocyte count of fresh water teleost, *Cirrhinus mrigala* (Ham), Biol. Med. 1 (2) (2009) 134–138.

[2] M. Thabet, A.A. El-Zomrawy, Degradation of acid red 17 dye with ammonium persulphate in acidic solution using photoelectrocatalytic methods, Arab. J. Chem. (in press), doi:10.1016/j.arabic.2011.03.001.

[3] S. Yang, P. Wang, X. Yang, L. Shan, W. Zhang, X. Shao, R. Niu, Degradation efficiencies of azo dye Acid Orange 7 by the interaction of heat, UV and anions with common oxidants: Persulfate, peroxymonosulfate and hydrogen peroxide, J. Hazard. Mater. 179 (2010) 552–558.

[4] M.R. Samarghandi, M. Zarrabi, A. Amrane, M.N. Sepehr, M. Noroozi, S. Namdari, A. Zarei, Kinetic of degradation of two azo dyes from aqueous solution by zero iron powder: Determination of the optimal conditions, Desalin. Water Treat. 40 (2012) 137–143.

[5] G.M. Nabil, N.M. El-Mallah, M.E. Mahmoud, Enhanced decolorization of reactive black 5 dye by active carbon sorbent-immobilized-cationic surfactant (AC-CS), J. Ind. Eng. Chem. 20 (2014) 994–1002.

[6] C.-H. Yu, C.-H. Wu, T.-H. Ho, P.K.A. Hong, Decolorization of C.I. reactive black 5 in UV/TiO_2, UV/oxidant and UV/TiO_2/oxidant system: A comparative study, Chem. Eng. J. 158 (2010) 578–583.

[7] E. Alvantosa-deLara, S. Barredo-Damas, M.I. Alcaina-Miranda, M.I. Iborra-Clar, Ultrafiltration technology with a ceramic membrane for reactive dye removal: Optimization of membrane performance, J. Hazard. Mater. 209–210 (2012) 492–500.

[8] U.D. Gul, G. Donmez, Application of mixed fungal biomass for effective reactive dye removal from textile effluents, Desalin. Water Treat. 51 (2013) 3597–3603.

[9] N. Dizge, C. Aydiner, E. Demirbas, M. Kobya, S. Kara, Adsorption of reactive dyes from aqueous solutions

by fly ash: Kinetic and equilibrium studies, J. Hazard. Mater. 150 (2008) 737–746.

[10] M.C. Yeber, L. Diaz, J. Fernandez, Catalytic activity of the SO_4^{-} radical for photogegradation of the azo dye Cibacron Brilliant Yellow 3 and 3,4-dichlorophenol: Optimization by application of response surface methodology, J. Photochem. Photobiol. A 215 (2010) 90–95.

[11] M. Klavarioti, D. Mantzavinos, D. Kassinos, Removal of residual pharmaceuticals from aqueous systems by advanced oxidation processes, Environ. Int. 35 (2009) 402–417.

[12] M.G. Antoniou, A.A. de la Cruz, D.D. Dionysiou, Degradation of microcystin-LR using sulfate radicals generated through photolysis, thermolysis and e^{-} transfer mechanisms, Appl. Catal. B: Environ. 96 (2010) 290–298.

[13] N. Daneshvar, M.H. Rasoulifard, A.R. Khataee, F. Hosseinzadeh, Removal of C.I. acid orange 7 from aqueous solution by UV irradiation in the presence of ZnO nanopowder, J. Hazard. Mater. 143 (2007) 95–101.

[14] Y.O. Seok, W.K. Hyeong, M.P. Jun, S.K. Hung, Y. Chohee, Oxidation of polyvinyl by persulfate activated with heat, Fe^{2+} and zero-valent ion, J. Hazard. Mater. 168 (2009) 346–351.

[15] G.R. Peyton, The free-radical chemistry of persulfate-based total organic carbon analyzers, Mar. Chem. 41 (1993) 91–103.

[16] C.-H. Yen, K.-F. Chen, C.-M. Cao, S.-H. Liang, Application of persulfate to remediate petroleum hydrocarbon-contaminated soil: Feasibility and comparison with common oxidants, J. Hazard. Mater. 186 (2011) 2097–2102.

[17] G.V. Buxton, C.L. Greenstock, W.P. Helman, A.B. Ross, Critical review of rate constants of reactions of hydrated electrons, hydrogen atoms and hydroxyl radicals ($^{\cdot}OH/O^{\cdot-}$) in aqueous solution, J. Phys. Chem. Ref. Data 17 (1988) 513–886.

[18] C. Tan, N. Gao, W. Chu, C. Li, M.R. Templeton, Degradation of diuron by persulfate activated with furrous ion, Sep. Purif. Technol. 95 (2012) 44–48.

[19] G.P. Anipsitakis, D.D. Dionysiou, Radical generation by the interaction of transition metals with common oxidants, Environ. Sci. Technol. 38 (2004) 3705–3712.

[20] J. Zhao, Y. Zhang, X. Quan, S. Chen, Enhanced oxidation of 4-chlorophenol using sulfate radicals generated from zero-valent iron and peroxydisulfate at ambient temperature, Sep. Purif. Technol. 71 (2010) 302–307.

[21] L.G. Devi, K.E. Rajashekhar, K.S.A. Raju, S.G. Kumar, Kinetic modeling based on the non-linear regression analysis for the degradation of Alizarin Red S by advanced photo Fenton process using zero valent metallic iron as the catalyst, J. Mol. Catal. A 314 (2009) 88–94.

[22] P. Gayathri, R.P.J. Dorathi, K. Palanivelu, Sonochemical degradation of textile dyes in aqueous solution using sulphate radicals activated by immobilized cobalt ions, Ultrason. Sonochem. 17 (2010) 566–571.

[23] A. Ghauch, A.M. Tuqan, N. Kibbi, S. Geryes, Methylene blue discoloration by heated persulfate in aqueous solution, Chem. Eng. J. 213 (2012) 259–271.

[24] S. Yang, X. Yang, X. Shao, R. Niu, L. Wang, Activated carbon catalyzed persulfate oxidation of Azo dye acid orange 7 at ambient temperature, J. Hazard. Mater. 186 (2011) 659–666.

[25] A.H. Gemeay, A.-F.M. Habib, M.A.B. El-Din, Kinetics and mechanism of the uncatalyzed and Ag(I)-catalyzed oxidative decolorization of Sunset Yellow and Ponceau 4R with peroxydisulphate, Dyes Pigm. 74 (2007) 458–463.

[26] G. Vishnu, S. Palanisamy, K. Joseph, Assessment of fieldscale zero liquid discharge treatment systems for recovery of water and salt from textile effluents, J. Clean. Prod. 16 (2008) 1081–1089.

[27] J. Fu, Y. Zhao, Q. Wu, Optimising photoelectrocatalytic oxidation of fulvic acid using response surface methodology, J. Hazard. Mater. 144 (2007) 499–505.

[28] P.D. Haaland, Statistical problem solving, in: P.D. Haaland (Ed.), Experimental Design in Biotechnology, Marcel Dekker, New York, NY, 1989, pp. 1–18.

[29] S. Ghafari, H.A. Aziz, M.H. Isa, A.A. Zinatizadeh, Application of response surface methodology (RSM) to optimize coagulation-flocculation treatment of leachate using poly-aluminum chloride (PAC) and alum, J. Hazard. Mater. 163 (2009) 650–656.

[30] A. Zuorro, M. Fidaleo, R. Lavecchia, Response surface methodology (RSM) analysis of photodegradation of sulfonated diazo dye Reactive Green 19 by UV/H_2O_2 process, J. Environ. Manage. 127 (2013) 28–35.

[31] B.K. Korbahti, M.A. Rauf, Response surface methodology (RSM) analysis of photoinduced decoloration of toluidine blue, Chem. Eng. J. 136 (2008) 25–30.

[32] M.A. Bezerra, R.E. Santelli, E.P. Oliveira, L.S. Villar, L.A. Escaleira, Response surface methodology (RSM) as a tool for optimization in analytical chemistry, Talanta 76 (2008) 965–977.

[33] A.I. Khuri, J.A. Cornell, Response Surfaces, Designs and Analysis, second ed., Marcel Dekker, New York, NY, 1996.

[34] S.-X. Li, D. Wei, N.-K. Mak, Z. Cai, X.-R. Xu, H.-B. Li, Y. Jiang, Degradation of diphenylamine by persulfate: Performance optimization, kinetics and mechanism, J. Hazard. Mater. 164 (2009) 26–31.

[35] E. Kusvuran, S. Irmak, H.I. Yavuz, A. Samil, O. Erbatur, Comparison of the treatment methods efficiency for decolorization and mineralization of reactive black 5 azo dye, J. Hazard. Mater. 119 (2005) 109–116.

[36] Y. Kacar, E. Alpay, V.K. Ceylan, Pretreatment of Afyon alcaloide factory's wastewater by wet air oxidation (WAO), Water Res. 37 (2003) 1170–1176.

[37] X.-R. Xu, X.-Z. Li, Degradation of azo dye Orange G in aqueous solutions by persulfate with ferrous ion, Sep. Purif. Technol. 72 (2010) 105–111.

[38] A. Loukanov, T. Rusnakov, N. Petrov, V. Blaskov, I. Stambolova, A. Angelov, S. Nakabayashi, Eco-friendly nanophotocatalysts for discoloring of azo dyes in industrial wastewaters, Annual of the University of Mining and Geology "ST. IVAN RILSKI" 54 (2011) 156–160.

[39] S. Chatterjee, S.-R. Lim, S.H. Woo, Removal of reactive black 5 by zero-valent iron modified with various surfactants, Chem. Eng. J. 160 (2010) 27–32.

[40] D.E. Kritikos, N.P. Xekoukoulotakis, E. Psillakis, D. Mantzavinos, Photocatalytic degradation of reactive black 5 in aqueous solutions: Effect of operating conditions and coupling with ultrasound irradiation, Water Res. 41 (2007) 2236–2246.

[41] C. Liang, C.-F. Huang, Y.-J. Chen, Potential for activated persulfate degradation of BTEX contamination, Water Res. 42 (2008) 4091–4100.

[42] C.-G. Niu, Y. Wang, X.-G. Zhang, G.-M. Zeng, D.-W. Huang, M. Ruan, X.-W. Li, Decolorization of an azo dye Orange G in microbial fuel cells using Fe(II)-EDTA catalyzed persulfate, Bioresour. Technol. 126 (2012) 101–106.

[43] S.-Y. Oh, S.-G. Kang, P.C. Chiu, Degradation of 2,4-dinitrotoluene by persulfate activated with zero-valent iron, Sci. Total Environ. 408 (2010) 3464–3468.

[44] S.-C. Xu, H.-D. Zhou, X.-Y. Wei, J. Lu, The pH dependence and effects of the oxidative products of some aromatic compounds in ozonation under UV irradiation, Ozone Sci. Eng. 11 (1989) 281–296.

[45] Z. Zuo, Y. Katsumura, Formation of hydrated electron and BrO_3 (radical from laser photolysis of BrO_3)-aqueous solution, J. Chem. Soc. Faraday Trans. 94 (1998) 3577–3580.

[46] S. Rodriguez, L. Vasquez, D. Costa, A. Romero, A. Santos, Oxidation of Orange G by persulfate activated by Fe(II), Fe(III) and zero valent iron (ZVI), Chemosphere 101 (2014) 86–92.

[47] S. Nam, P.G. Tratnyek, Reduction of azo dye with zero-valent iron, Water Res. 34 (1999) 1837–1845.

[48] M.C. Chang, H.Y. Shu, H.H. Yu, An integrated technique using zero-valent iron and UV/H_2O_2 sequential process for complete decolorization and mineralization of CI Acid Black 24 wastewater, J. Hazard. Mater. 138 (2006) 574–581.

[49] J. Cao, L. Wei, Q. Huang, L. Wang, S. Han, Reducing degradation of azo dye by zero-valent iron in aqueous solution, Chemosphere 38 (1999) 565–571.

[50] W. Feng, D. Nansheng, H. Helin, Degradation mechanism of azo dye C.I. reactive red 2 by iron powder reduction and photooxidation in aqueous solutions, Chemosphere 41 (2000) 1233–1238.

[51] T. Satapanajaru, C. Chompuchan, P. Suntornchot, P. Pengthamkeerati, Enhancing decolorization of reactive black 5 and Reactive Red 198 during nano zerovalent iron treatment, Desalination 266 (2011) 218–230.

[52] R.E. Huie, C.L. Clifton, P. Neta, Electron transfer reaction rates and equilibria of the carbonate and sulfate radical anions, Int. J. Radiat. Appl. Ins. Part C. Radiat. Phys. Chem. 38 (5) (1991) 477–481.

[53] C.J. Liang, Z.S. Wang, N. Mohantry, Influences of carbonate and chloride ions on persulfate oxidation of trichloroethylene at 20℃, Sci. Total Environ. 370 (2006) 271–277.

[54] Y. Wu, S. Zhou, F. Qin, X. Ye, Modeling physical and oxidative removal properties of Fenton process for treatment of landfill leachate using response surface methodology (RSM), J. Hazard. Mater. 180 (2010) 456–465.

[55] A.M. Joglekar, A.T. May, Product excellence through design of experiments[J], Cereal Foods Word 32 (1987) 857–868.

[56] M.Y. Nordin, V.C. Venkatesh, S. Sharif, S. Elting, A. Abdullah, Application of response surface methodology in describing the performance of coated carbide tools when turning AISI 104 steel, J. Mater. Process. Technol. 145 (2004) 46–58.

[57] B.K. Korbahti, Response surface optimization of electrochemical treatment of textile dye wastewater, J. Hazard. Mater. 145 (2007) 277–286.